inventions

MDPI

Article

Parametric Optimization of Entropy Generation in Hybrid Nanofluid in Contracting/Expanding Channel by Means of Analysis of Variance and Response Surface Methodology

Ahmad Zeeshan [1], Rahmat Ellahi [1,2,3,*], Muhammad Anas Rafique [1], Sadiq M. Sait [4,5] and Nasir Shehzad [1]

[1] Department of Mathematics and Statistics, International Islamic University Islamabad, Islamabad 92521, Pakistan; ahmad.zeeshan@iiu.edu.pk (A.Z.); nasir.shehzad.vt@iiu.edu.pk (N.S.)
[2] Department of Mechanical Engineering, University of California Riverside, Riverside, CA 92521, USA
[3] Center for Modeling & Computer Simulation, Research Institute, King Fahd University of Petroleum & Minerals, Dhahran 31261, Saudi Arabia
[4] Department of Computer Engineering, King Fahd University of Petroleum & Minerals, Dhahran 31261, Saudi Arabia; sadiq@kfupm.edu.sa
[5] Interdisciplinary Research Center for Smart Mobility and Logistics, King Fahd University of Petroleum & Minerals, Dhahran 31261, Saudi Arabia
* Correspondence: rellahi@alumni.ucr.edu

Abstract: This study aims to propose a central composite design (CCD) combined with response surface methodology (RSM) to create a statistical experimental design. A new parametric optimization of entropy generation is presented. The flow behavior of magnetohydrodynamic hybrid nanofluid (HNF) flow through two flat contracting expanding plates of channel alongside radiative heat transmission was considered. The lower fixed plate was externally heated whereas the upper porous plate was cooled by injecting a coolant fluid with a uniform velocity inside the channel. The resulting equations were solved by the Homotopic Analysis Method using MATHEMATICA 10 and Minitab 17.1. The design consists of several input factors, namely a magnetic field parameter (M), radiation parameter (N) and group parameter (Br/A1). To obtain the values of flow response parameters, numerical experiments were used. Variables, especially the entropy generation (Ne), were considered for each combination of design. The resulting RSM empirical model obtained a high coefficient of determination, reaching 99.97% for the entropy generation number (Ne). These values show an excellent fit of the model to the data.

Keywords: entropy generation; parametric optimization; analysis of variance; response surface methodology

Citation: Zeeshan, A.; Ellahi, R.; Rafique, M.A.; Sait, S.M.; Shehzad, N. Parametric Optimization of Entropy Generation in Hybrid Nanofluid in Contracting/Expanding Channel by Means of Analysis of Variance and Response Surface Methodology. *Inventions* **2024**, *9*, 92. https://doi.org/10.3390/inventions9050092

Academic Editors: Alexander Klimenko and Eugen Rusu

Received: 25 May 2024
Revised: 19 July 2024
Accepted: 22 August 2024
Published: 27 August 2024

1. Introduction

Entropy generation is a measure of the irreversibility of thermal energy. This plays a crucial part in engineering applications, especially in design and heat transfer optimization. It is defined as a measure of thermal disorder or randomness. Entropy generation is frequently related to irreversible processes in thermodynamics, where energy is lost to heat or other forms of energy that cannot fully be transformed back to useful work. The second law of thermodynamics, which states that the total entropy of an isolated system either rises or stays constant but never falls, governs this idea. Entropy generation is the process by which a closed system's overall dissipation is calculated over time [1–5]. Every physical process and every thermodynamic operation involve some energy dissipation, an increase in disorder and an increase in entropy. Also, to analyze the charter of important parameters, such as entropy, changes may occur with some parameters and may not change with some other parameters. Sensitivity analysis is a valuable method for calculating this effect in fluid dynamics. With this methodology, an empirical quadratic order providing a correlation between input parameters and entropy generation is called for when performing numerical

simulation and experimental analysis [6–9]. Methods based on modern AI techniques, such as Artificial Neural Networks (ANNs) and Response Surface Methodology (RSM), are used to obtain empirical models [10]. RSM is the most commonly used statistical technique when many input factors affect a particular performance index or quality attribute. Statistical experimental methods are important in industrial and engineering design and simulation works. Sensitivity analysis is an important method in science and engineering, especially for complex system engineering issues. It identifies areas of emphasis for system design to ensure robustness and correctness across multiple inputs by conducting diagnostic modeling and simulations. Sensitivity analysis has been employed to study the effects of changing viscosity and thermal conductivity on flow performance metrics [11], including the Nusselt number and skin friction coefficient over a permeable wedge. Here, the author concluded that skin friction was the most sensitive to the suction parameter among the others involved. Whereas, the Nusselt number shows variation in thermal conductivity. In Ref. [12], the authors investigated the sensitivity analysis of nanofluids including nanoparticles and motile bacteria. The results depicted that skin friction was more sensitive towards the Brownian motion parameter and the Sherwood parameter showed high sensitivity due to the Lewis number. Meanwhile, Ref. [13] investigated the sensitivity analysis of Cu–water nanofluid-forced convection over a wedge. The author confirmed from the results that optimal conditions for skin friction and the Nusselt number arose for M = 0.62, a wedge angle of 166.72 and a nanoparticle concentration of 0.052. Also, Ref. [14] delved into the sensitivity analysis of various physical input quantities in solar heat exchangers and concluded that the Richardson number, diameter of nanoparticles and wall surface emissivity positively influenced the Nusselt number in a solar heat exchanger. In Ref. [15], the sensitivity and optimization of hybrid nanofluid heat transfer was investigated. Parametric optimization using RSM for the boundary layer flow of ethylene glycol-based ZnO nanoliquid over a moving wedge was investigated in [16]. Meanwhile, Ref. [17] conducted numerical and sensitivity analyses of three-dimensional flow and heat transfer of a nanoliquid over a wedge and concluded that a higher pressure gradient and shear-to-strain rate but lower Lewis number were found to be the best conditions in which the heat transfer rate was maximized. A vast amount of the literature exists on the sensitivity analysis of boundary value problems [18–21]. By conducting a sensitivity analysis, it is possible to determine what variables, such as the skin friction coefficient, Nusselt number and Sherwood number, have a significant impact on flow performance metrics. This information can be used to focus on these critical aspects and analyze the stability of corresponding effective parameters on flow behavior.

Furthermore, nanofluids exhibit significantly higher thermal conductivity than regular fluids due to the effective suspension of metallic nanoparticles in the base fluid. Since then, several mathematical models have been developed to better understand and enhance the thermal conductivity of nanofluids [22–30].

The aim of this study is to provide a central composite design combined with Response Surface Methodology to create a statistical experimental design. A new parametric optimization of entropy generation is presented. The flow behavior of magnetohydrodynamic hybrid nanofluid flow in an expanding/constricting channel alongside radiative heat transmission was taken into account. The sensitivity of variables related to the flow is presented by means of Response Surface Methodology (RSM) and the statistical method called Analysis of Variance (ANOVA). This study is not yet available in the existing literature.

2. Mathematical Modelling

The flow geometry is shown in Figure 1. The forces applied on the flow were the uniform and transverse magnetic field. An externally heated lower wall (T_0) of the channel is represented along the x-axis. In order to cool down the upper wall to temperature (T_1), a coolant fluid through the upper wall with a uniform velocity v_w was injected. The channel expanded and contracted with respect to the time function b(t).

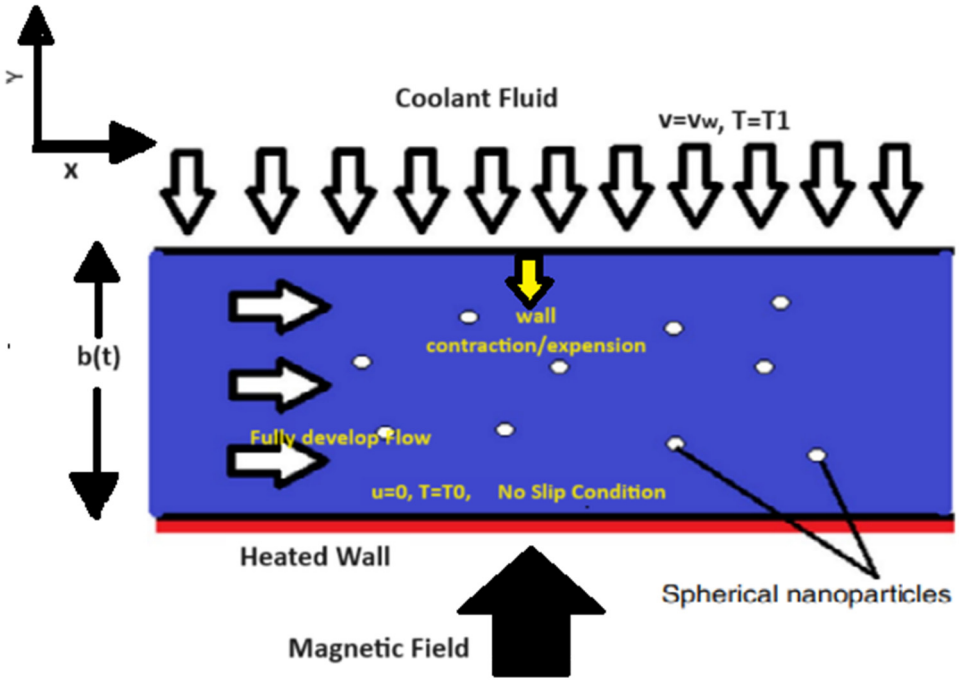

Figure 1. Flow geometry of the problem.

Both the fluid phase and nanoparticles were considered to be in a thermally stable state, exhibiting no velocity for sliding along the wall.

2.1. Governing Equations

The momentum and energy equations can be written in vector form as the following:

$$\rho\left(\frac{\partial \mathbf{V}}{\partial t} + \mathbf{V}.\nabla\mathbf{V}\right) = -\nabla p + \mu\nabla^2\mathbf{V} + \frac{1}{3}\mu\nabla(\nabla.\mathbf{V}) + \mathbf{F} \tag{1}$$

$$\rho\left[\frac{\partial h}{\partial t} + \nabla.(h\mathbf{V})\right] = -\frac{Dp}{Dt} + \nabla.(k\nabla T) + \phi \tag{2}$$

where h is the enthalpy and ϕ represents dissipation. The respective boundary conditions are

$$u = 0,\ T = T_0 \text{ at lower wall} \tag{3}$$

$$u = 0,\ T = T_1,\ v = v_w \text{ at upper wall moving with velocity } \dot{b}(t) \tag{4}$$

The stream function is introduced as

$$\tilde{\psi} = \frac{v\tilde{x}}{b}\tilde{F}(\eta, t), \tilde{v} = -\frac{v}{b}\tilde{F}, \tilde{u} = \frac{v\tilde{x}}{b^2}\tilde{F}_\eta, \tag{5}$$

where $= \tilde{y}/b$.

The non-dimensional resulting equations [31] take the following forms:

$$F_{\eta\eta\eta\eta} + \frac{B_1}{B_2}((\alpha\eta + ReF)F_{\eta\eta\eta} + (3\alpha - ReF_\eta)F_{\eta\eta}) - \frac{B_5}{B_2}M^2F_{\eta\eta} = 0. \tag{6}$$

$$\begin{aligned} &B_4Ec\left(f_{\eta\eta} + x^2g_{\eta\eta}\right) + B_3Br(\alpha\eta + ReF)\left(f_\eta + x^2g_\eta\right) + B_5BrM^2ReF_\eta^2x^2 \\ &+B_2BrRe\left(4F_\eta^2 + x^2F_{\eta\eta}^2\right) + \frac{4}{3}N\left(f_{\eta\eta} + x^2g_{\eta\eta}\right) = 0, \end{aligned} \tag{7}$$

where $N = \frac{4\sigma^* T_\infty^3}{k^*_{hnf} k_f}$ is the radiation parameter. The coefficient of the terms was equated including with and without x^2 of Equation (7).

The associated boundary conditions are

$$F(0) = 0,\ F_\eta(0) = 0,\ F_\eta(1) = 0,\ F(1) = 1. \tag{8}$$

$$\left.\begin{array}{r} \text{at } \eta = 0,\ f = g = 0, \\ \text{at } \eta = 1, \quad f = \dfrac{1}{Ec}, \quad g = 0. \end{array}\right\} \tag{9}$$

The mathematical Equations (6) and (7) subject to boundary conditions (8) and (9) were solved with the help of the Homotopic Analysis Method [32–35] and the series solutions were obtained as

$$F = F_0(\eta) + \sum_{m=1}^{k} F_m(\eta), \tag{10}$$

$$\theta = \theta_0(\eta) + \sum_{m=1}^{k} \theta_m(\eta). \tag{11}$$

2.2. Entropy Generation

In this section, a comprehensive research study of the parametric optimization for flow performance, and specifically the entropy generation number for the flow of hybrid nanofluid in an expanding/contracting channel, is presented.

The equation of entropy of the hybrid nanofluid [31] is written as

$$\begin{aligned} S'''_{gen} = {} & \frac{k_{hnf}}{T^2}\left(1 + \frac{16\sigma^*_{hnf} T_\infty^3}{3k^*_{hnf}}\right)\left[\left(T_{\tilde{x}}\right)^2 + \left(T_{\tilde{y}}\right)^2\right] \\ & + \frac{\mu_{hnf}}{T_1}.\left[2\left(\tilde{v}_{\tilde{y}}\right)^2 + 2\left(\tilde{u}_{\tilde{x}}\right)^2 + \left(\tilde{u}_{\tilde{y}}\right)^2 + \left(\tilde{v}_{\tilde{x}}\right)^2 + 2\left(\tilde{u}_{\tilde{y}}\right)^2\left(\tilde{v}_{\tilde{x}}\right)^2\right] + \frac{\sigma_{hnf}}{T_1} B_0^2 \tilde{u}^2, \end{aligned} \tag{12}$$

$$Ne = \frac{S'''_{gen}}{S_{gen}} = B_4 Ec^2\left(1 + \frac{4}{3}N\right)\left(f_\eta^2 + 2x^2 f_\eta g_\eta\right) + B_2\left(\frac{Br}{A1}\right)Re.\left(2\left(F_\eta^2 + F^2\right) + x^2 F_{\eta\eta}^2\right) + \frac{Br}{A1} B_5 M x^2 F_\eta^2, \tag{13}$$

where $S_{gen} = \frac{k_f (T_2 - T_1)^2}{b^2 T_1^2}$. The total energy of the system described in (12) can also be written as

$$Ne = N_H + N_f + N_m. \tag{14}$$

Here, N_H constitutes the entropy generated by heat transfer, N_f constitutes the entropy generated by fluid friction and N_m constitutes the entropy generated by the magnetic field force.

3. Results

In this section, the sensitivity analysis results are presented. To explore the flow of a hybrid nanofluid across a channel, the statistical method known as Analysis of Variance (ANOVA) will be used to compare the means of two or more groups or treatments.

3.1. Response Surface Methodology (RSM)

In order to manage enormous datasets in research and engineering, statistical experimental design is crucial. Using the entropy generation number and other output reactions to establish empirical correlations between input parameters is essential.

We used the Central Composite Design (CCD) to build our experimental design since it is efficient at tolerating three input factors. To obtain the corresponding output values for each response variable, namely the magnetic field parameter (M), radiation parameter (N) and group parameter (Br/A1), we utilized the bvp4c routine in MATLAB (Version with bvp4c solver). The input parameters A, B and C were represented using symbolic

notation, while the coefficients of the entropy generation number (Ne) were also used. The general quadratic functions of Ne based on principles of the RSM are defined in [36]. With the use of these functions, we were able to create mathematical representations by using input parameters and the intended result variables, providing a useful tool for additional analysis and optimization.

$$\mathrm{Ne} = \beta_0 + \beta_1 \mathrm{A} + \beta_2 \mathrm{B} + \beta_3 \mathrm{C} + \beta_{11} \mathrm{A}^2 + \beta_{22} \mathrm{B}^2 + \beta_{33} \mathrm{C}^2 + \beta_{12} \mathrm{AB} + \beta_{13} \mathrm{AC} + \beta_{23} \mathrm{BC}, \quad (15)$$

where $\beta_0, \beta_1, \beta_2, \ldots, \beta_{23}$ are coefficients of Ne.

3.2. ANOVA

ANOVA partitions the total variation in a dataset into variation between groups and variation within groups. It is used to determine what terms in an empirical correlation have a significant effect on the output quantities. The sequential F-test was applied with twenty-one runs to construct the regression model's fit, and the selection and rejection of terms in the model were based on large values of F and small values of p ($p < 0.05$). It can be conducted as a one-way ANOVA when comparing multiple independent groups or as a two-way ANOVA when studying the effects of two independent factors. Assumptions of ANOVA include the normal distribution of data within groups, equal variances and the independence of observations. To improve the estimated regression and statistical analysis of experimental models, simulation studies were conducted using various experimental substances, and residual plots were formed using ANOVA. It is widely employed in research fields such as psychology, biology, economics and social sciences. It provides a powerful tool for hypothesis testing and investigating differences between groups, allowing researchers to draw meaningful conclusions from their data.

3.3. Development of Empirical Correlation

The reliability of Response Surface Methodology (RSM) in determining the input variables on response quantities such as the entropy generation number were investigated. During the sensitivity analysis, residual error and lack of fit were considered, with a residual error indicating the regression lines of unexplained data points and lack of fit occurring when the model failed to capture the relationship between the input variables and response quantities. A three-level face-centered CCD-RSM was taken into consideration. Design input variables with their CCD levels are presented in Table 1.

Table 1. Design input parameters and their levels.

Input Parameter	Coding Symbol	Level		
		−1	**0**	**1**
M	A	0	0.75	1.5
N	B	0.1	0.115	0.13
Br/A	C	0	1.75	3.5

A three-level face-centered CCD-RSM was used with minimum, central and maximum values of −1, 0 and 1, respectively. Nineteen degrees of freedom (DOFs) with twenty runs were suitable for constructing the design as shown in Table 2. The table was drawn using Minitab.

Table 2. Design of experiments and response results.

Experiment Runs	Point Type	Coded Value			Real Value			Output Response
		A	B	C	M	N	Br/A1	Ne
1	Factorial	−1	1	−1	0.00	0.13	0.000	77.174
2		1	1	−1	1.50	0.13	0.000	78.939
3		−1	−1	−1	0.00	0.1	0.000	98.673
4		1	−1	−1	1.5	0.1	0.000	101.367
5		−1	1	1	0.0	0.13	3.5	92.380
6		1	1	1	1.5	0.13	3.5	94.345
7		−1	−1	1	0.00	0.1	3.5	113.879
8		1	−1	1	1.5	0.1	3.5	116.773
9	Axial	−1	0	0	0.00	0.115	0.175	76.422
10		1	0	0	1.50	0.115	0.175	77.508
11		0	1	0	0.75	0.13	0.175	85.541
12		0	−1	0	0.75	0.1	0.175	107.596
13		0	0	−1	0.75	0.115	0.000	69.192
14		0	0	1	0.75	0.115	3.5	84.443
15–20	Central	0	0	0	0.75	0.115	0.175	76.817

The *p*-value evaluates a model's accuracy, the F-value measures the range of values around the average value. The F-values in Table 3 display that the model was statistically significant for the entropy generation number.

Table 3. Analysis of variance (ANOVA).

	Source	DOF	AdjSS	AdjMS	F-Value	*p*-Value
Ne	Model	9	3768.32	418.70	6720.47	0.000
	Linear	3	1803.67	601.22	9650.07	0.000
	Square	3	1964.20	654.73	10,508.93	0.000
	Interaction	3	0.45	0.15	2.42	0.127
	Error	10	0.62	0.06	-	-
	Lack of Fit	5	0.62	0.12	-	-
	Pure Error	5	0.000	0.000	-	-
	Total	19	3768.94	-	-	-

The RSM model's coefficient of determination (R^2) was 99.98% for Ne. The adjusted coefficient of determination (Adj R^2) for Ne was 99.97%. These statistics (R^2 and Adj (R^2)) also give the surety of the fit goodness. Table 4 presents the entropy generation regression coefficient. A large *p*-value is not statistically significant and represents that altering the input value will not affect the output results. Meanwhile, a low *p*-value ($p < 0.05$) is considered statistically significant and those values that obtained this criterion were retained in the model, while those that did not were eliminated.

$$\mathrm{Ne} = 76.8209 + 1.0404\mathrm{A} + 10.9910\mathrm{B} + 7.6474\mathrm{C} + 19.742\mathrm{B}^2 + 0.2323\mathrm{AB}. \quad (16)$$

Table 4. Regression analysis for Ne.

Term	Coefficient	*p*-Value	
	Ne		
Constant	76.8209	0.000	
A	1.0404	0.000	
B	10.9910	0.000	
C	7.6474	0.000	
A^2	0.138	0.379	Not significant
B^2	19.742	0.000	
C^2	−0.009	0.954	Not significant
AB	0.2323	0.025	
AC	0.0500	0.583	Not significant
BC	0.0001	0.999	Not significant
-	$R^2 = 99.98\%$	$AdjR^2 = 99.97\%$	

3.4. Sensitivity Analysis of the Pertained Parameter

The use of sensitivity analysis in engineering problems is a common technique to determine how changing parametric values affects the desired outcomes. This approach particularly gives suitable results when trying to identify the impact of multiple influential factors. Sensitivity analysis predicts the outcome of a decision by analyzing a relevant set of parameters. To analyze the sensitivity of the pertained parameters, the derivatives of Equation (15) were taken and the tabulated form of empirical correlation was obtained.

$$\frac{\partial \mathrm{Ne}}{\partial \mathrm{A}} = 1.0404 + 0.2323\mathrm{B}, \tag{17}$$

$$\frac{\partial \mathrm{Ne}}{\partial \mathrm{B}} = 10.9910 + 39.448\mathrm{B} + 0.2323\mathrm{A}, \tag{18}$$

$$\frac{\partial \mathrm{Ne}}{\partial \mathrm{C}} = 7.6474. \tag{19}$$

Figure 2 indicates that the data were continuous with the frequency focused on zero which represents the numerical data following the normal probability distributions of a bell-shaped plot. Figure 3 shows that the empirical correlation was more symmetrical and less distorted. Figure 4 indicates that as the number of observations increased, the residual decreased, which showed a strong connection between the fitted and original values. To estimate the goodness of fit also discussed by and which data had high numerical values, as shown in Table 4, a strong correlation between the input variables and Ne was observed.

Table 5 outlines the variations in output response quantities. The sensitivity of entropy generation Ne at $C = 0$, with symbols A and B varying according to Table 5, was observed. Figures 5–7 provide a graphical view of the sensitivity analysis of the output response parameters of (Ne) with bar charts indicating the response. The effects of the input variables' magnetic field (M), radiation parameter (Ne) and group parameter (Br/A) are indicated in Figures 5–7. In Figures 5–7, the effects of input variables on entropy generation (Ne), where A and B are dominant parameters, are also represented. Furthermore, Ne was positively sensitive to all three parameters. This means that increasing the radiation parameter (N) enhanced the response of entropy generation (Ne), as discussed in Table 5. Also, it means that entropy increased with a change in all the parameters, but the change was rapid with the rise in radiation parameters, and minimum variation was observed with the change in a magnetic field. Entropy also showed sensitivity to the group parameters.

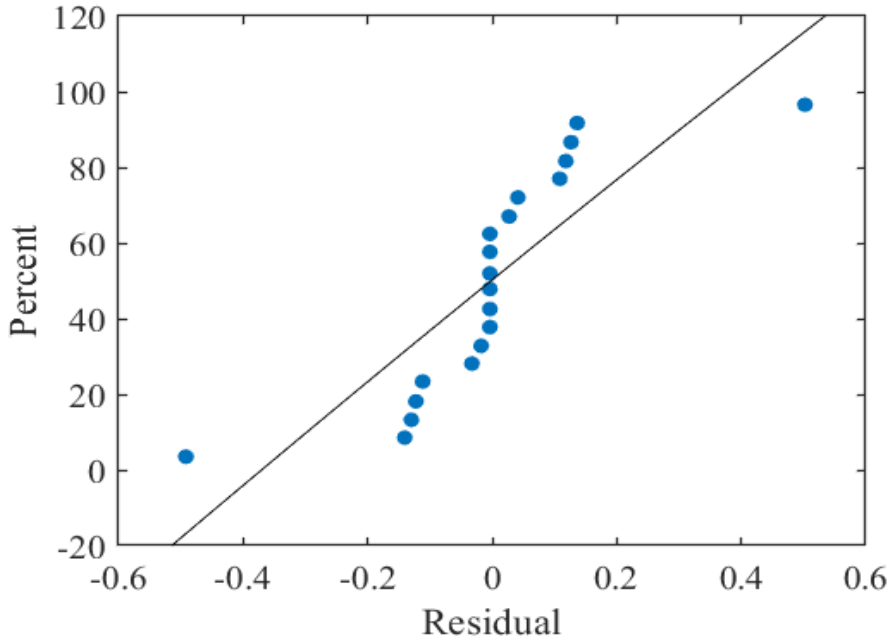

Figure 2. Normal probability graph of the total energy of Ne.

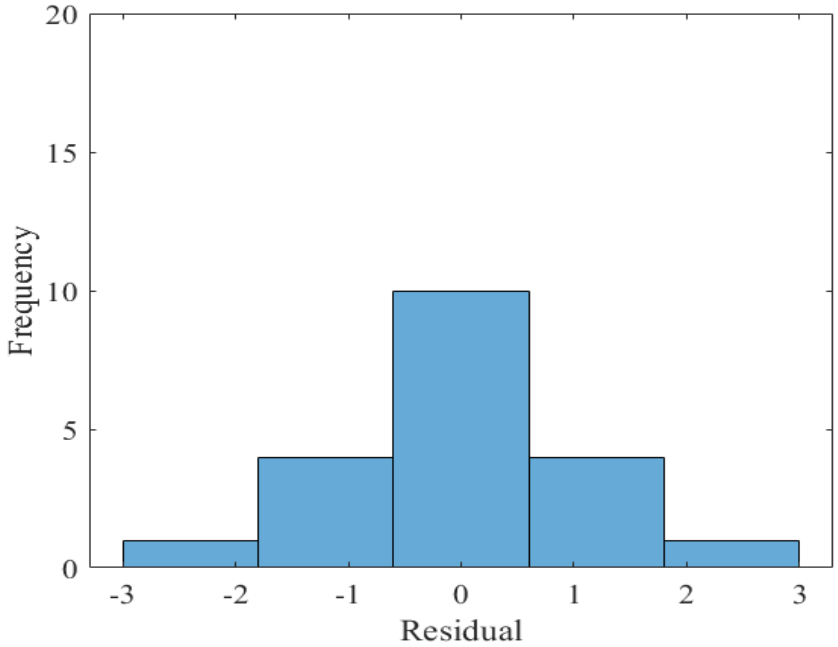

Figure 3. Histogram of the empirical correlation of Ne.

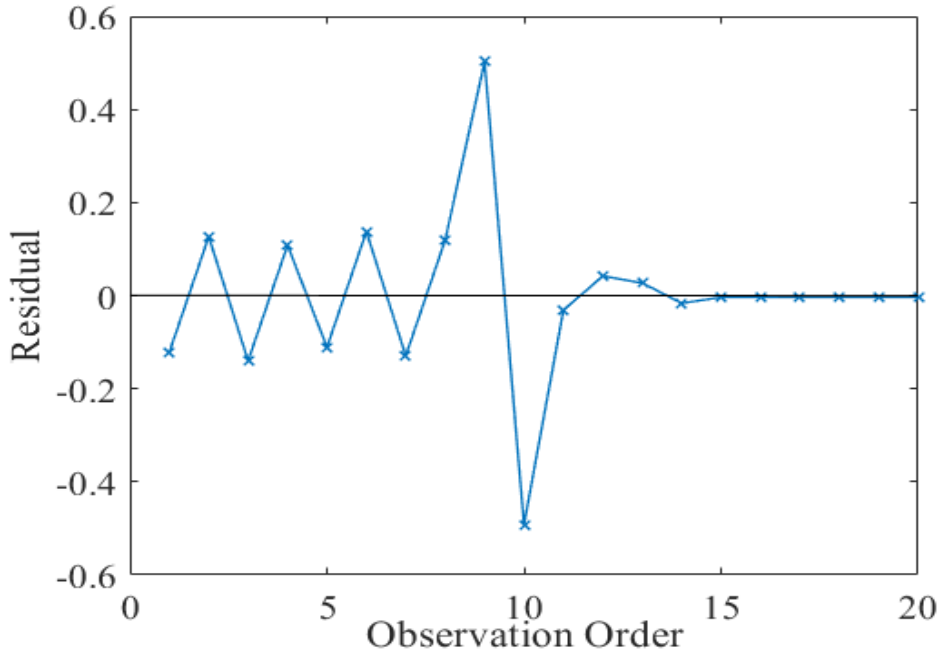

Figure 4. Observation order against standardized residual plot of Ne.

Table 5. Sensitivity of Ne.

A	B	$\frac{\partial Ne}{\partial A}$	$\frac{\partial Ne}{\partial B}$	$\frac{\partial Ne}{\partial C}$
−1	−1	1.06363	14.9394	7.6474
	0	1.067114	15.53166	7.6474
	1	1.070599	16.12392	7.6474
0	−1	1.06363	15.11362	7.6474
	0	1.067114	15.70588	7.6474
	1	1.070599	16.29814	7.6474
1	−1	1.06363	15.28785	7.6474
	0	1.067114	15.88011	7.6474
	1	1.070599	16.47237	7.6474

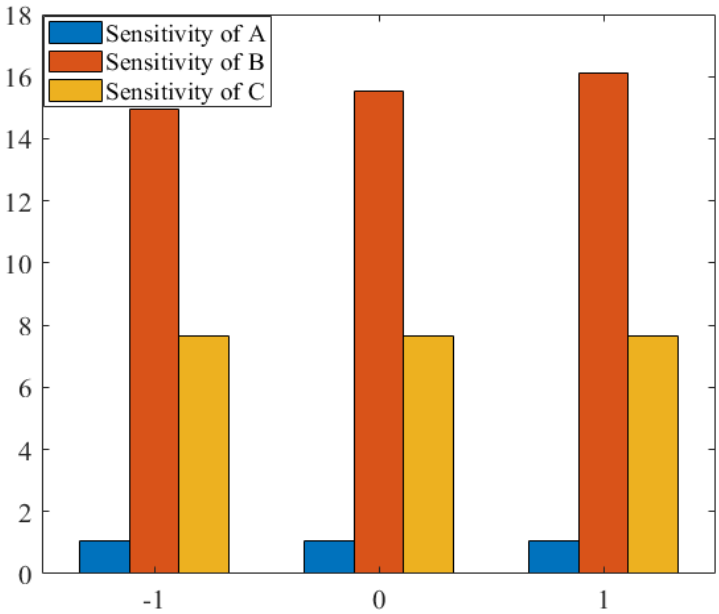

Figure 5. Sensitivity analysis at C at the central level and A at the lower level for Ne.

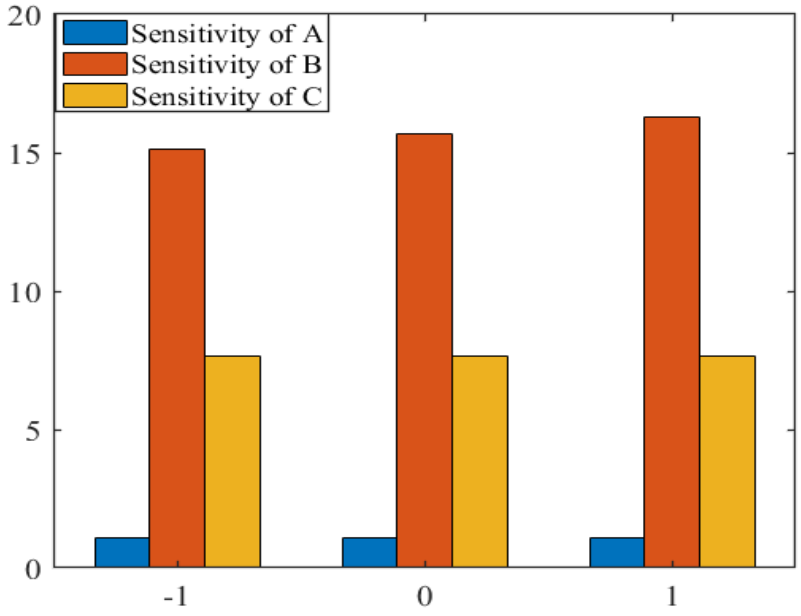

Figure 6. Sensitivity analysis at C at the central level and A at the central level for Ne.

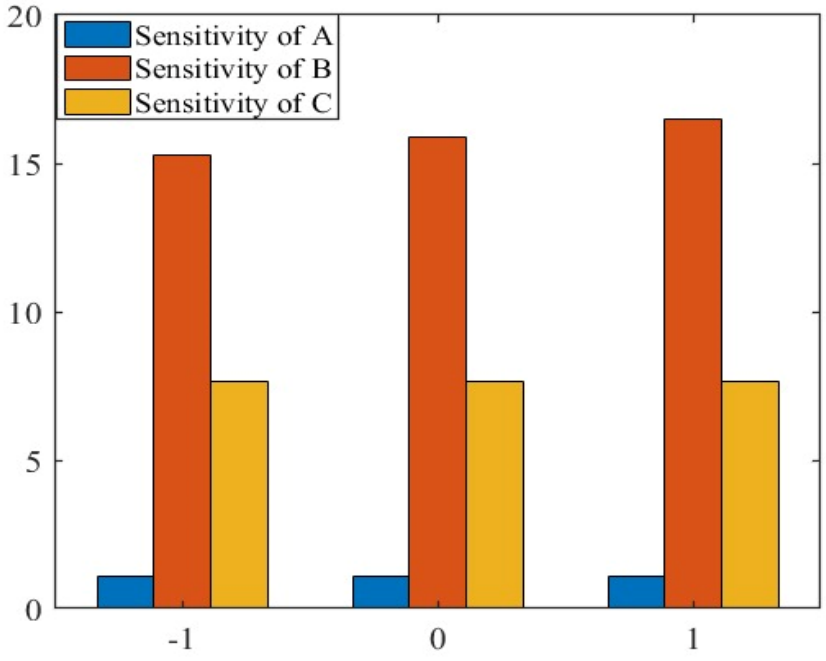

Figure 7. Sensitivity analysis at C at the central level and A at the upper level for Ne.

Sensitivity analysis is useful in limiting the discussion of the non-uniqueness of a solution to changing the sensitivity parameters only.

4. Conclusions

This study provides a comprehensive sensitivity analysis of the entropy generation of nanofluid flow on expanding/contracting channels. Sensitivity analysis is an engineering tool that helps to improve the understanding of input parameters with respect to output response, leading to effective decision-making. The effects of factors such as magnetic field parameters, radiation parameters and group parameters were investigated. To obtain a deeper understanding of the flow dynamic, an empirical correlation was developed by using response surface methodology to examine the sensitivity of the flow response parameters. The critical observations of this study are listed as the following:

1. The sensitivity analysis identified that the radiation parameter was the most influential in the flow.
2. It was found that by increasing radiation parameters, entropy generation increased.
3. It was noted that the group parameter had a significant role in determining the flow behavior.

Author Contributions: Conceptualization, A.Z.; supervision, R.E.; investigation, M.A.R.; validation, N.S.; formal analysis, S.M.S.; writing—original draft, M.A.R.; writing—review and editing, S.M.S. All authors have read and agreed to the published version of the manuscript.

Funding: This research received no external funding.

Data Availability Statement: Data are contained within the article.

Conflicts of Interest: The authors declare no conflicts of interest.

Nomenclature

b(t)	Expand or contract function
b_0	Initial channel height
B_i, i = 1, 2, 3, 4, 5	Constant parameters in hybrid nanofluids
α	Expansion ratio
f (η), g(η)	Compositional form of temperature
k^*_{nf}	Mean absorption coefficient of the hybrid nanofluid
M	Magnetic parameter
N	Radiation parameter
σ^*	Stefan Boltzmann constant
Λ	Wall permeability
Pr	Prandtl number
p^*	Dimensional pressure
p	Non-dimensional pressure
Re	Reynold number
Br	Brinkman number
Ec	Eckert number
t	Time
T	Temperature
T_1	Temperature at the lower plate
T_2	Temperature at the upper plate
u^-	Dimensional velocity in the x direction
u	Non-dimensional velocity in the x direction
$\bar{v}$	Dimensional velocity in the y direction
V	Non-dimensional velocity in the y direction
F	Stream function variable
θ	Temperature
A1	Temperature difference
ϕ_1, ϕ_2	Nanoparticle volume fractions
S'''_{gen}	Entropy generation
Ne	Non-dimensional total entropy generation
Br/A_1	Group parameter
N_H	Entropy generated by heat transfer
N_f	Entropy generated by fluid friction
N_m	Entropy generated by the magnetic field force
A, B, C	Regression parameters
β_i, i = 0, 1, 2,3, 11, 22, 33, 12, 13, 23	Regression coefficient for Ne
Subscripts	
F	Host fluid
hnf	Hybrid nanofluid
P	Particle

References

1. Zhang, L.; Bhatti, M.M.; Marin, M.; Mekheimer, K.S. Entropy analysis on the blood flow through anisotropically tapered arteries filled with magnetic zinc-oxide (ZnO) nanoparticles. *Entropy* **2020**, *22*, 1070. [CrossRef]
2. Jamalabadi, M.Y.A.; Safaei, M.R.; Alrashed, A.A.A.A.; Nguyen, T.K.; Filho, E.P.B. Entropy generation in thermal radiative loading of structures with distinct heaters. *Entropy* **2017**, *19*, 506. [CrossRef]
3. Ellahi, R.; Alamri, S.Z.; Basit, A.; Majeed, A. Effects of MHD and slip on heat transfer boundary layer flow over a moving plate based on specific entropy generation. *J. Taibah Univ. Sci.* **2018**, *12*, 476. [CrossRef]
4. Bhatti, M.M.; Abbas, T.; Rashidi, M.M.; Ali, M.E.-S. Numerical simulation of entropy generation with thermal radiation on MHD carreau nanofluid towards a shrinking sheet. *Entropy* **2016**, *18*, 200. [CrossRef]
5. Bhatti, M.M.; Abbas, T.; Rashidi, M.M.; Ali, M.E.-S.; Yang, Z. Entropy generation on MHD Eyring–Powell nanofluid through a permeable stretching surface. *Entropy* **2016**, *18*, 224. [CrossRef]
6. Hemmat Esfe, M.; Alidoust, S.; Mohammadnejad Ardeshiri, E.; Kamyab, M.H.; Toghraie, D. Experimental study of rheological behavior of MWCNT-Al2O3/SAE50 hybrid nanofluid to provide the best nano-lubrication conditions. *Nanoscale Res. Lett.* **2022**, *17*, 4. [CrossRef]
7. Esfe, M.H.; Arani, A.A.A.; Esfandeh, S. Improving engine oil lubrication in light-duty vehicles by using of dispersing MWCNT and ZnO nanoparticles in 5W50 as viscosity index improvers (VII). *Appl. Therm. Eng.* **2018**, *143*, 493–506. [CrossRef]
8. Abdulrahman, A. Modeling and optimization of dynamic viscosity of copper nanoparticles dispersed in gear oil using response surface methodology. *Mater. Today Proc.* **2021**, *42*, 771–775. [CrossRef]
9. Kole, M.; Dey, T.K. Role of interfacial layer and clustering on the effective thermal conductivity of CuO–gear oil nanofluids. *Exp. Therm. Fluid Sci.* **2011**, *35*, 1490–1495. [CrossRef]
10. Gürel, A.E.; Ağbulut, Ü.; Biçen, Y. Assessment of machine learning, time series, response surface methodology and empirical models in prediction of global solar radiation. *J. Clean. Prod.* **2020**, *277*, 122353. [CrossRef]
11. Hussain, D.; Asghar, Z.; Zeeshan, A.; Alsulami, H. Analysis of sensitivity of thermal conductivity and variable viscosity on wall heat flux in flow of viscous fluid over a porous wedge. *Int. Commun. Heat Mass Transf.* **2022**, *135*, 106104. [CrossRef]
12. Chan, S.Q.; Aman, F.; Mansur, S. Sensitivity analysis on thermal conductivity characteristics of a water-based bionanofluid flow past a wedge surface. *Math. Probl. Eng.* **2018**, *2018*, 9410167. [CrossRef]
13. Vahedi, S.M.; Pordanjani, A.H.; Raisi, A.; Chamkha, A.J. Sensitivity analysis and optimization of MHD forced convection of a Cu-water nanofluid flow past a wedge. *Eur. Phys. J. Plus* **2019**, *134*, 124. [CrossRef]
14. Shirvan, K.M.; Mamourian, M.; Mirzakhanlari, S.; Ellahi, R. Two phase simulation and sensitivity analysis of effective parameters on combined heat transfer and pressure drop in a solar heat exchanger filled with nanofluid by RSM. *J. Mol. Liq.* **2016**, *220*, 888–901. [CrossRef]
15. Mahanthesh, B.; Shehzad, S.A.; Mackolil, J.; Shashikumar, N.S. Heat transfer optimization of hybrid nanomaterial using modified Buongiorno model: A sensitivity analysis. *Int. J. Heat Mass Transf.* **2021**, *171*, 121081. [CrossRef]
16. Mahanthesh, B.; Mackolil, J.; Mallikarjunaiah, S.M. Response surface optimization of heat transfer rate in Falkner-Skan flow of ZnO−EG nanoliquid over a moving wedge: Sensitivity analysis. *Int. Commun. Heat Mass Transf.* **2021**, *125*, 105348. [CrossRef]
17. Rana, P.; Gupta, G. Numerical and sensitivity computations of three-dimensional flow and heat transfer of nanoliquid over a wedge using modified Buongiorno model. *Comput. Math. Appl.* **2021**, *101*, 51–62. [CrossRef]
18. Darbari, B.; Rashidi, S.; Abolfazli Esfahani, J. Sensitivity analysis of entropy generation in nanofluid flow inside a channel by response surface methodology. *Entropy* **2016**, *18*, 52. [CrossRef]
19. Sheremet, M.A.; Grosan, T.; Pop, I. Natural convection and entropy generation in a square cavity with variable temperature side walls filled with a nanofluid: Buongiorno's mathematical model. *Entropy* **2017**, *19*, 337. [CrossRef]
20. Safaei, M.R.; Ahmadi, G.; Goodarzi, M.S.; Shadloo, M.S.; Goshayeshi, H.R.; Dahari, M. Heat transfer and pressure drop in fully developed turbulent flows of graphene nanoplatelets–silver/water nanofluids. *Fluids* **2016**, *1*, 20. [CrossRef]
21. Goodarzi, M.; Tlili, I.; Tian, Z.; Safaei, M.R. Efficiency assessment of using graphene nanoplatelets-silver/water nanofluids in microchannel heat sinks with different cross-sections for electronics cooling. *Int. J. Numer. Methods Heat Fluid Flow* **2020**, *30*, 347–372. [CrossRef]
22. Turkyilmazoglu, M. An analytical treatment for the exact solutions of MHD flow and heat over two–three dimensional deforming bodies. *Int. J. Heat Mass Transf.* **2015**, *90*, 781–789.
23. Kanwal, A.; Khan, A.A.; Sait, S.M.; Ellahi, R. Heat transfer analysis of magnetohydrodynamics peristaltic fluid with inhomogeneous solid particles and variable thermal conductivity through curved passageway. *Int. J. Numer. Methods Heat Fluid Flow* **2024**, *34*, 1884. [CrossRef]
24. Ellahi, R.; Hussain, F.; Abbas, S.A.; Sarafraz, M.M.; Goodarzi, M.; Shadloo, M.S. Study of two-phase newtonian nanofluid flow hybrid with hafnium particles under the effects of slip. *Inventions* **2020**, *5*, 6. [CrossRef]
25. Zeeshan, A.; Hussain, D.; Asghar, Z.; Bhatti, M.M.; Duraihem, F.Z. Thermal optimization of MHD nanofluid over a wedge by using response surface methodology: Sensitivity analysis. *Propuls. Power Res.* **2023**, *12*, 556–567.
26. Chamkha, A.J.; Jena, S.K.; Mahapatra, S.K. MHD convection of nanofluids: A review. *J. Nanofluids* **2015**, *4*, 271–292.
27. Bhatti, M.M.; Bég, O.A.; Ellahi, R.; Doranehgard, M.H.; Rabiei, F. Electro-magnetohydrodynamics hybrid nanofluid flow with gold and magnesium oxide nanoparticles through vertical parallel plates. *J. Magn. Magn. Mater.* **2022**, *564*, 170136.

28. Gibanov, N.S.; Sheremet, M.A.; Oztop, H.F.; Al-Salem, K. MHD natural convection and entropy generation in an open cavity having different horizontal porous blocks saturated with a ferrofluid. *J. Magn. Magn. Mater.* **2018**, *452*, 193–204.
29. Zafar, S.; Khan, A.A.; Sait, S.M.; Ellahi, R. Numerical investigation on unsteady compressible flow of viscous fluid with convection under the effect of Joule heating. *J. Comput. Appl. Mech.* **2024**, *55*, 423–439.
30. Rizwan, M.; Hassan, M.; Makinde, O.D.; Bhatti, M.M.; Marin, M. Rheological modeling of metallic oxide nanoparticles containing non-newtonian nanofluids and potential investigation of heat and mass flow characteristics. *Nanomaterials* **2022**, *12*, 1237. [CrossRef]
31. Zeeshan, A.; Khan, M.I.; Ellahi, R.; Asghar, A.Z. Artificial neural network simulation and sensitivity analysis for optimal thermal transport of magnetic viscous fluid over shrinking wedge via RSM. *Int. J. Numer. Methods Heat Fluid Flow* **2023**, *33*, 3492–3518. [CrossRef]
32. Ellahi, R.; Zeeshan, A.; Shahzad, N.; Hussain, A.; Sait, S.M. Mixed convection of two layers with radiative electro-magnetohydrodynamics nanofluid flow in vertical enclosure. *Nanotechnology* **2024**, *35*, 095402. [CrossRef]
33. Liao, S.J. An analytic approximate technique for free oscillations of positively damped systems with algebraically decaying amplitude. *Int. J. Non-Linear Mech.* **2003**, *38*, 1173–1183. [CrossRef]
34. Ellahi, R. The effects of MHD and temperature dependent viscosity on the flow of non-Newtonian nanofluid in a pipe: Analytical solutions. *Appl. Math. Model.* **2013**, *37*, 1451–1457. [CrossRef]
35. Hussain, F.; Ellahi, R.; Zeeshan, A. Mathematical models of electro magnetohydrodynamic multiphase flows synthesis with nanosized Hafniump particles. *Appl. Sci.* **2018**, *8*, 275. [CrossRef]
36. Srinivas, S.; Reddy, A.S.; Ramamohan, T.R. A study on thermal-diffusion and diffusion-thermo effects in a two-dimensional viscous flow between slowly expanding or contracting walls with weak permeability. *Int. J. Heat Mass Transf.* **2012**, *55*, 3008–3020. [CrossRef]